

OPTIMIZATION OF THE GEOMETRIC PARAMETERS OF A TWISTED TAPE FOR THE INTENSIFICATION OF HEAT TRANSFER IN SOLAR COLLECTOR

Silva Junior, L. G.

Leandro O. Salviano¹

luis.goncalves@unesp.br

leandro.salviano@unesp.br¹

Energy Engineering, São Paulo State University

Department of Mechanical Engineering, São Paulo State University¹

Av. Barrageiros, 1881, Rosana, SP, 19.274-000, Brazil

Av. Brasil, 56, Ilha Solteira, SP, 15.385-000, Brazil¹

Abstract. Large is the amount of thermal energy that needs to be supplied for the heating of water in domestic or industrial environments, whether by burning gas, biomass or by direct use of electricity. Today, these traditional methods have been resisted in their expansion in response to the inexorable increase in demand. In this sense, solar energy has emerged as one of the most attractive renewable sources for this type of application, requiring, in this way, the continuous technological development of solar collectors more efficient thermally that meet the application requirements. Thus, the objective of this paper is to perform the numerical simulation of the process of intensification of heat transfer in a flat plate solar collector with active system and indirect circulation of single-phase working fluid, through the device known as Twisted Tape, down Reynolds number 600. The geometric parameters of the twisted tape subjected to the Direct Optimization approach are: Twisting tape pitch (P), length (L), Translate (T) and twisted tape radius (R1 and R2). The analysis of the optimization process associated to the heat transfer intensification performance and the associated pressure loss were analyzed through computational modeling in ANSYS and ESTECO ModeFrontier software. The main results of this project indicate that the optimization process using the Genetic Algorithm method led to a geometry with asymmetric radius for both the Reynolds number evaluated, yielding significant results corresponding to a global heat transfer increase of approximately 170 %, while the symmetric tape with twist ratio 4 (R4) increased by 52 %. Evaluating the flow loss, the optimized tapes again showed better performance as they increased the pressure loss by about 248 %, while the symmetrical (R4) tapes increased by 268 % for Reynolds 600.

Keywords: Solar Energy, Genetic Algorithm, Twisted Tape, Heat Transfer, Solar Collector, Optimization

1 Introduction

The use of fossil fuels are the most common in the world, a fact that entails a great demand of them for the supply of global energy needs [1]. Although these petroleum-based fuels, coal and natural gas are very effective sources of energy and have a positive impact in the economic context, they have a negative impact on the environment and human health [2]. The excessive use of fossil fuels to supply the world's energy consumption is responsible for the high emission of polluting gases such as CO₂ and consequently global warming [3]. In this way, the Kyoto Protocol was created to mitigate greenhouse gases and increase the use of renewable energies [4]. In addition, the scarcity of fossil resources has intensified the demand for new renewable sources due to higher energy demand than supply [5]. The use of solar energy in homes in California, USA reduced or avoided approximately 696 metric tons of CO₂ emissions through the installation of about 113 solar systems [6]-[7], the solar energy has domestic and industrial applications and can supply considerably the energy consumption required. In Greece, it is estimated that the average consumption of all residences is 10.2 MWh of thermal energy, for heating environments, hot water production, cooking and 3.75 MWh of electricity for the various appliances [8] in another study, estimates that 15% of the energy required in industries in Europe is for heating processes [9]. Within this aspect, solar thermal energy emerges as a potential player among renewable energies to supply the energy consumption due to the generation of free, clean and affordable energy [1], as well as relieve pressure on scarce sources and provide heat where there are no other sources of available energy [10].

The solar collector is the main equipment in a solar thermal energy application and can be found of different types, however, in this journal the flat plate solar collector is studied, which is the most frequently used and found in homes [11]. The manifold consists of a clear cover, an absorbent plate, tubes, insulation and a working fluid. Its function is to absorb the solar radiation and transfer the converted heat to a working fluid, in this case, to the water. Although solar heating in solar collectors is not a new technique, the increase of the transfer of heat and consequently of its efficiency is still a challenge [11].

The solar water collector considered in this work is an active system for a single-phase fluid. One of the most applied passive techniques to improve the heat transfer is the twisted tape inserts in the tubes, which can be seen in several works [12]–[21] and are distinguished by the development of swirls in the flow which increase the perturbation of the boundary layer of flow in the tube, in addition to increasing the fluid mixture which due to axial velocity enhances the heat transfer and also develops spiral flow lines which create a larger flow path. [22]. However, although twisted tapes promote heat transfer they also entail significant pressure loss, as analyzed in an experimental study by Kumar & Prasad [23] the use of twisted tape in a solar collector increased heat transfer by 18% while the pressure loss increased by 87% compared to a flat tube.

This paper demonstrates the numerical simulation of the process of intensification of heat transfer in a flat plate solar collector by means of the Twisted Tape device, for Reynolds number 600, using a model of solar collector base used in social projects of the Brazilian government, popularly found in residences. The geometric parameters of the twisted tape subjected to the Direct Optimization approach are: Twisting tape pitch (P), length (L), Translate (T) and twisted tape radius (R1 and R2). The analysis of the optimization process associated to the heat transfer intensification performance and the associated pressure loss were analyzed through computational modeling in ANSYS and ESTECO ModeFrontier software. The main results indicate that the optimization process using the Genetic Algorithm method led to a geometry with asymmetric radius for both the Reynolds number evaluated, yielding significant results corresponding to a global heat transfer increase of approximately 170 %, while the symmetric twist ratio tape 4 (R4) increased by 52 %. By evaluating the flow pressure loss, the optimized tapes showed better performance because they increased the pressure loss by about 248 %, while the symmetrical (R4) tapes increased by 268 %.

2 Computational Methodology

2.1 Governing Equations

The numerical modeling of heat transfer and fluid flow within a circular tube is considered to be three-dimensional, incompressible, laminar and steady-state flow [24]. The fluid used is water, so the conditions for a Newtonian fluid are considered, where the respective equations are of continuity, momentum and energy.

$$\frac{\partial}{\partial x_j}(\rho u_j) = 0 \quad (1)$$

$$\frac{\partial}{\partial x_j}(\rho u_j u_i - \tau_{ij}) = -\frac{\partial p}{\partial x_i} \quad (2)$$

$$\frac{\partial}{\partial x_j} \left(\rho u_j h - k \frac{\partial T}{\partial x_j} \right) = -u_j \frac{\partial p}{\partial x_j} + \tau_{ij} \frac{\partial u_i}{\partial x_j} \quad (3)$$

A third-order convection scheme designed from the original MUSCL (Monotone Upstream-Centered Schemes for Conservation Laws) was used which improves the spatial potential of the mesh [25]. For the flow solution, the coupled algorithm was used which solves the continuity equations based on momentum and pressure. The gradients were evaluated by the gradient method based on Green Gauss Nodes where the nodal values are constructed from the weighted average of the values of the cells around the nodes, following the approach originally proposed by Holmes and Connel [26] and Rauch et al [27]. Computational convergence is established for residues smaller than 10^{-4} for the Momentum equation and 10^{-7} for the Energy equation.

2.2 Thermo - Hydraulic Parameters

The flow in the tube was characterized by its Reynolds number and calculated as a function of the pipe diameter, Eq. (4). The parameters for calculating heat transfer and pressure loss are expressed by the Nusselt number and the Friction factor, respectively, defined by equations 5 and 6.

$$Re = \frac{\rho u D}{\mu} \quad (4)$$

$$Nu = \frac{h D}{k} \quad (5)$$

$$f = \frac{2 \Delta P D}{\rho u^2 L_t} \quad (6)$$

The pressure loss ΔP (Eq. (7)) is the pressure difference between the input and the output of the computational domain:

$$\Delta P = \bar{P}_{in} - \bar{P}_{out} \quad (7)$$

Where,

$$\bar{P} = \frac{\iint_A p dA}{\iint_A dA} \quad (8)$$

The coefficient of convective heat transfer is determined according to Eq. (9):

$$h = \frac{q''}{(T_w - T_m)} \quad (9)$$

Finally, the temperatures are evaluated according to Eq. (10).

$$\bar{T} = \frac{\iint_A uT dA}{\iint_A u dA} \quad (10)$$

2.3 Computational domain and boundary conditions

The solar collector considered is like a commercial system used in homes assisted by governmental social projects, which have pipes with a diameter of 9.52 mm and a length of 1000 mm. For the proposed modeling, the thickness in the tube can be disregarded as a function of the boundary condition adopted and the characteristic of the heat transfer by conduction in the tube wall. For the construction of the twisted tape, two important geometric characteristics were considered for the process of intensification of the heat transfer, the first being the Half-pitch (W), which consists of the length of the tube in which the tape completes 180 ° of revolution, and the Twist Ratio (Y) defined as the ratio of the half-pitch and the inner diameter of the tape [28].

$$Y = \frac{W}{D} \quad (11)$$

The twisted tape of the design was constructed with 8 mm diameter, 64 mm pitch (twist ratio equivalent to 4), these being the initial defined conditions that will be submitted to the optimization process, in order to identify the optimal configuration of the parameterized factors, which are: Twist tape pitch (P), length (L), translate (T) and the tape radius (R1 and R2). Figure 1 illustrates the optimization parameters and Fig. 2 shows the constructed geometry of the solar collector tube with the twisted tape and the boundary conditions.

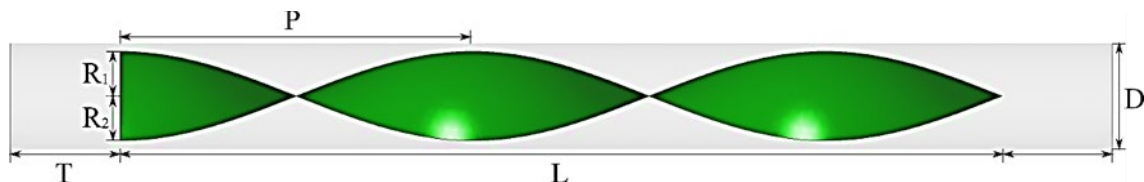


Figure 1. Representation of the twisted tape with the indication of the geometric parameters

The prescribed velocity corresponding to Reynolds 600 is adopted as a boundary condition at the input of the computational domain (Inlet). Heat Flux is imposed as a boundary condition on the pipe surface and equal to 750 W/m². At the exit of the domain is imposed the condition of prescribed pressure (Outlet). Figure 2 shows the contour conditions in the computational domain of the tube with the twisted tape inserted.

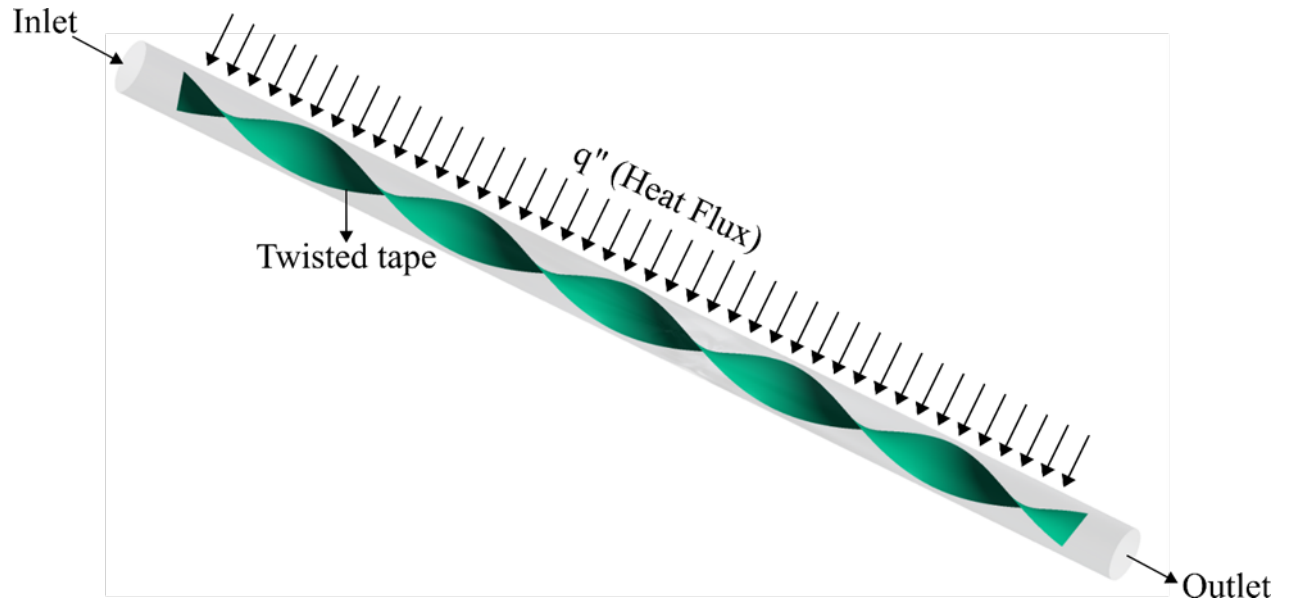


Figure 2. Computational domain with twisted tape

2.4 Grid independence and numerical validation

For the analysis of mesh independence, the Grid Convergence Index (GCI) method was used, which is based on the Richardson extrapolation method and aims to measure the relative error of the computational domain discretization. The method estimates numerical uncertainty by analyzing three sets of meshes with different refinements. As recommended in [29], it is desirable that the ratio factor between the meshes Eq. (12) be greater than or equal to 1.3:

$$r = \left(\frac{h_{fine}}{h_{course}} \right)^{\frac{1}{3}} \quad (12)$$

Where: h_{fine} represents the number of elements of the most refined mesh and h_{course} is the number of elements of the coarser mesh.

The parameters submitted to the GCI method, which characterize the thermohydraulic problem, are the friction factor and Nusselt number, which are calculated from the numerical solution of the flow inside the tube. In Table 1 we can analyze the three different grid thicknesses evaluated.

Table 1. Characteristics of the meshes and results of the GCI method

Mesh	Number of elements	Ratio Factor, r
Grid 1	433,724	*
Grid 2	1,270,877	1.43
Grid 3	2,800,472	1.3

The GCI (%) results indicated that the numerical uncertainty of the model as a function of the mesh refining is significantly small (0.054% for the friction factor and 2.07% for the Nusselt number), showing that the use of the Grid 2 is the most suitable option, since it has a small variation of the thermo-hydraulic parameters and a considerably smaller amount of elements than Grid 3, which reduces the time of convergence. Thus, the mesh independence was satisfactorily achieved by the GCI method.

Table 2. Numerical uncertainty of the model

Thermal-Hydraulic Parameter	GCI (%)
Nusselt Number	2,07
Friction Factor	0,054

The mesh method used was that of tetrahedron mesh due to its versatility and ability to model irregular domains. The quality of the mesh elements generated was analyzed by means of the Orthogonal Quality tool, which is calculated considering the vector normal to each face of the tetrahedron. The cosines between the faces are calculated by defining the orthogonality of the mesh, which must be minimum for good quality. Therefore, the closer the value is to 1, the better the quality of the tetrahedron mesh generated. Thus, the average value of mesh quality for Grid 2 was 0.87652, which is appropriate to use it. Figure 3 shows the mesh corresponding to Grid 2 in the computational domain, while Figure 4 shows the front part of the domain with the mesh.

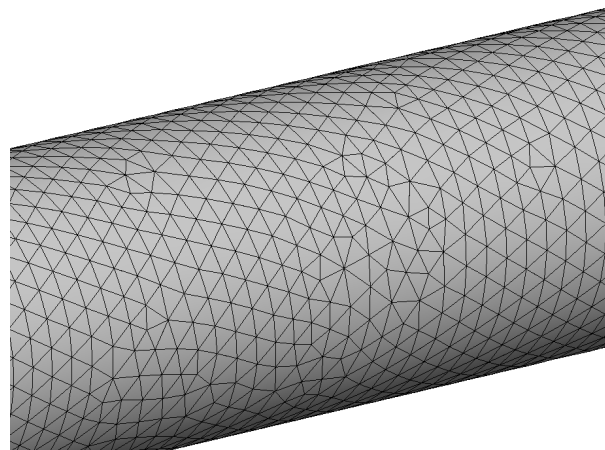


Figure 3. Details of the mesh generated on the tube

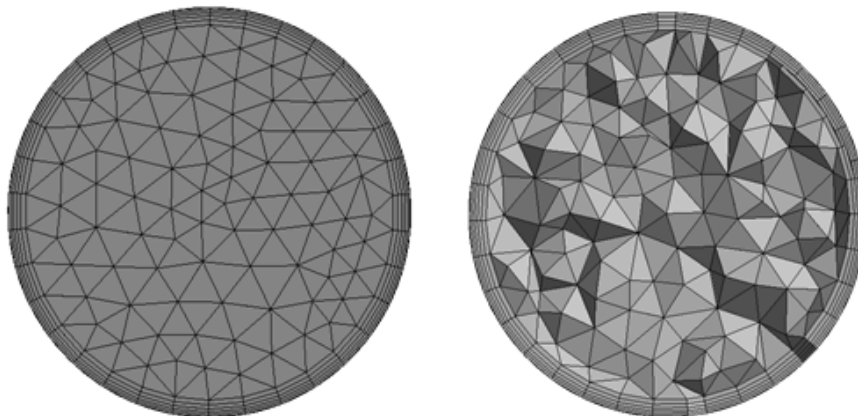


Figure 4. Details of the prism layers and tetrahedral elements for a cross section along the tube

For the numerical validation, a smooth tube was considered under fully developed flow hypothesis. The fully developed flow assessment was performed by analyzing the velocity profiles at the inlet and outlet regions of the tube by means of successive iterations (looping). Thus, after some looping the velocity profile becomes constant, satisfying the conditions for the fully developed flow. For a fully developed flow condition and under constant heat flux, as verified in the literature [30], the

Nusselt number value is equal to 4.36 and the value of the friction factor is a function of the Reynolds number ($f = \frac{64}{Re_D}$). Table 3 shows the results obtained in the simulation related to the theoretical values, so it can be analyzed that the numerical model robustly represents the analytical results with a small percentage difference.

Table 3. Validation correlation data of the numerical model

	Correlation	Simulation	Error (%)
Friction, f	0,107	0,104	2,43 %
Nusselt, Nu	4,360	4,485	2,86 %

2.5 Optimization process

In the optimization process, the five input variables described in Fig. 1 (Length, Translate, Pitch, Radius 1 and Radius 2) are submitted to the Direct Optimization approach. In this approach the very numerical model of the flow inside the tubes of the flat solar collector is admitted as the "objective function" to be optimized and, therefore, there are no errors of approximation.

Figure 5 shows the general outline of the flowchart applied to the Direct Optimization approach, where the optimal solution is found directly in a single step through the coupling of the numerical model of the flat solar collector and the optimization algorithm.

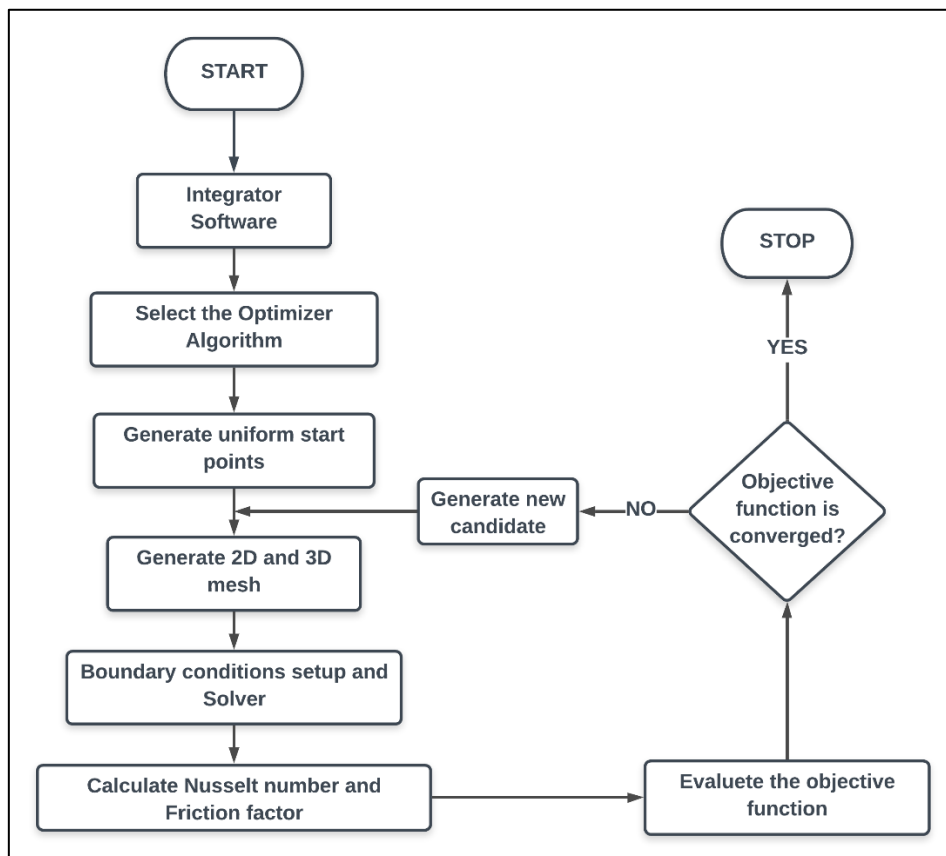


Figure 5. Flowchart applied to the Direct Optimization approach [31]

The choice of the objective function is governed by the nature of the problem to be treated, defined as a relation between the heat transfer and the associated loss of pressure (Nuf), as shown in Eq. (13). Thus, the geometric parameters are submitted to the method of optimization with the aim of maximizing the Nuf function.

$$Nuf = \frac{\left(\frac{Nu}{Nu_0}\right)}{\left(\frac{f}{f_0}\right)} \quad (13)$$

The optimization method used was known as the Genetic Algorithm (GA) evolution method, applied and discussed in several works as Holland [32-33], Goldberg [34], Michalewicz [35] e Fleming, P. J., & Purshouse, R. C [36]. One of the main advantages of this method is the ability to explore possible global and local optimum points. The ESTECO ModeFrontier PHD software was used to perform the optimization process. One of the main potentialities of this software is its ability to integrate the numerical simulation steps and the optimization method, allowing flexibility in the calculation of several thermohydraulic parameters directly in its interface.

For the direct optimization approach, operational ranges were defined for the five input geometric parameters considering the geometric constraints. Table 4 indicates the corresponding operating ranges.

Table 4. Predefined operating ranges for geometric parameters

Parameters	Operating Range (mm)	
	Lower	Upper
Length	300	990
Pitch	5	500
Radius 1	0.5	4
Radius 2	0.5	4
Translate	5	500

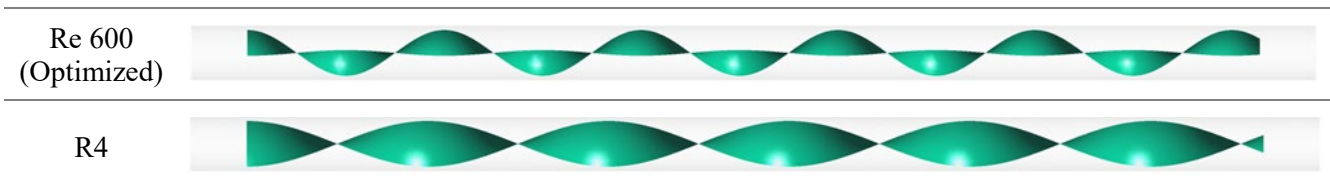
3 Results and discussion

The numerical simulation was performed in ANSYS software 18.2. The results obtained by means of the optimization process for the Reynolds in question were compared with the twisted tape of twisted ratio 4 (R4), which is frequently used in several applications in order to intensify heat transfer. Table 5 shows the configurations of the optimized models and the twisted tape R4. Note that the R4 setting is used for both Reynolds numbers. In order to evaluate the process of heat transfer in each configuration, the Nusselt (Nu) ratio of the twisted tape on the Nusselt of the smooth tube (Nu_0) is used. Similarly, to evaluate the pressure loss process, the ratio of the friction factor (f) of the flow with the twisted tape to the friction factor of the smooth pipe (f_0) is used.

Table 5. Twisted tapes configuration

	Length (mm)	Pitch (mm)	Rad. 1 (mm)	Rad. 2 (mm)	Translate (mm)
Re 600 (Optimized)	900	35	4	0.5	20
R4	980	64	4	4	10

Table 6. Geometrical configurations of the optimized twisted tapes and R4



In Fig. 6, the twisted tape optimized for Reynolds 600 enhances the global heat transfer by approximately 170 %, while R4 intensified only 52%. The increase in pressure loss associated with the heat transfer enhancement process was 248 % for the optimized tape and 268 % for R4. In this way, it is possible to analyze that the optimized configurations demonstrated better performance with an excellent result evidencing increase in heat transfer and reduction in the loss of pressure when compared with the twisted ratio tape 4.

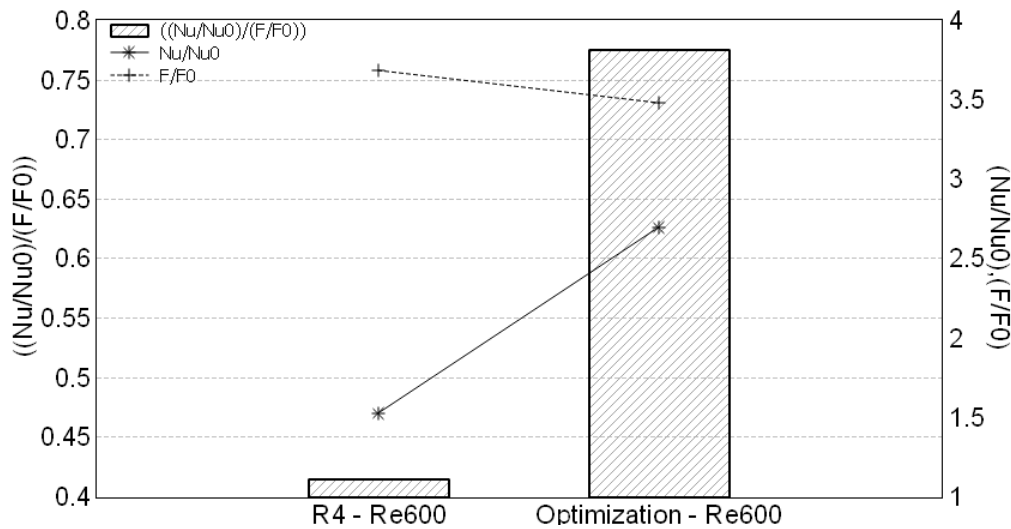


Figure 6. Ratio between the heat transfer and Friction factor.

Another factor that can be observed in Fig. 11 is the ratio between the Nusselt number and the friction factor (Nu_f), which allows to analyze the thermo-hydraulic performance that characterizes the relation between the heat transfer and the associated pressure loss. Thus, for values greater than 1, the intensification of the heat transfer is greater than the penalty in the associated pressure loss, indicating a greater effectiveness of this passive technique.

The results show that the optimized tapes produced better performance in relation to the R4 configuration, representing 78% of the intensification of the heat transfer in the increase of the pressure loss for Reynolds 600 and 41% for the tape R4. These considerably positive results generated by the optimized tapes are inherent in the configuration of the parameters created by the optimization process, such as the identified asymmetry of the radius, the pitch with shorter length increasing the distortions in the flow and the length of the twisted tape.

Figure 7 illustrate the impacts generated by the passive devices in the Nusselt number values along the tube, while Figures 8, demonstrate the behavior of the pressure loss along the tube.

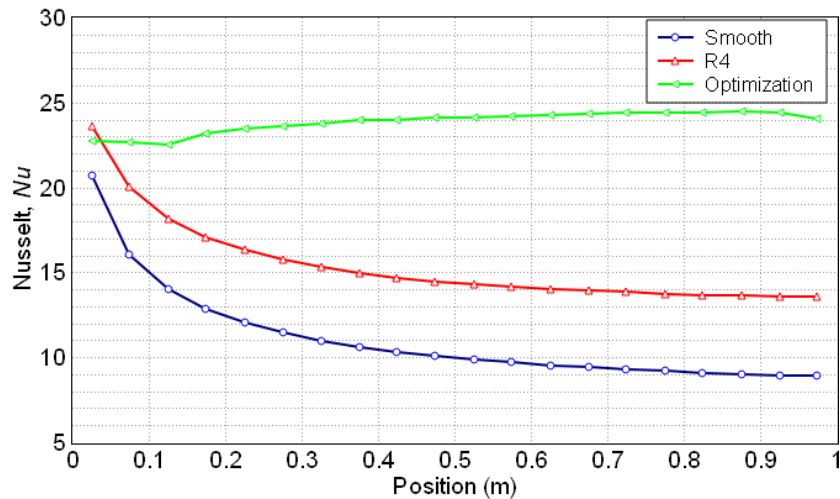


Figure 7. Behavior of the Nusselt number along the tube.

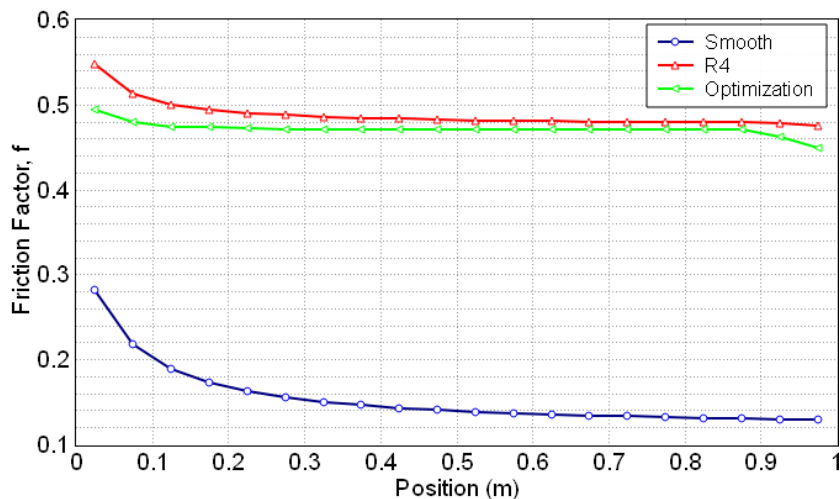


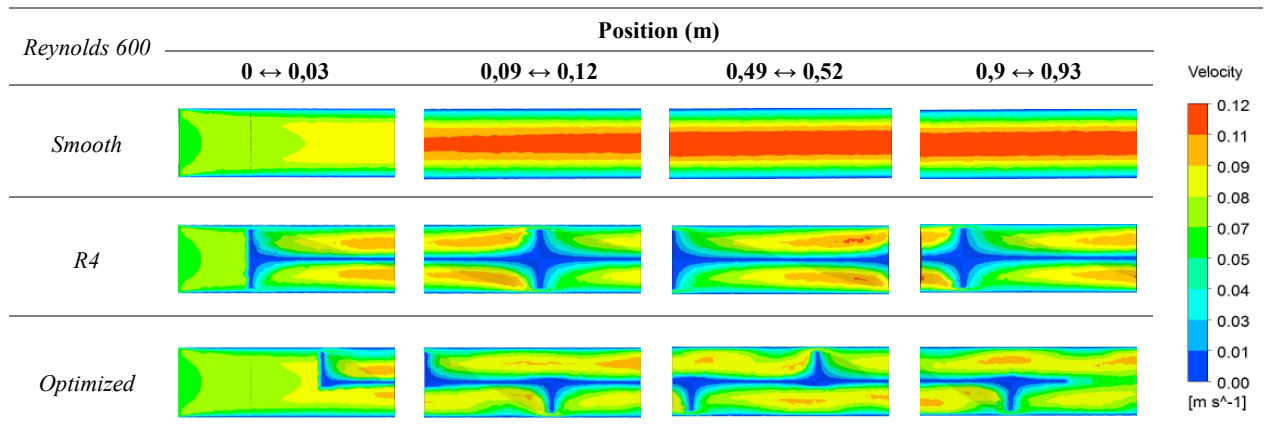
Figure 8. Profile of the Friction factor along the tube.

According to the previous graphs, it is possible to note the impact of the twisted tapes in the increase of the heat transfer and the increase in the flow loss of the flow, especially for the asymmetric tapes. It is noted that the development of the boundary layer at the start of the tube results in the greater heat transfer because of the higher property gradients, although it is decreasing as a function of the growth of the boundary layer thickness. This behavior is interrupted by the optimized twisted tape, which due to its asymmetry presents progressive increase in heat transfer.

Figure 8 show the behavior of the pressure loss along the tube. one can identify an affinity between the behavior of the optimized tape and the R4 tape, which is due to the similarity between its configurations, especially to the tape lengths that are similar, however, it can be verified that the optimized tape still has a smaller impact on the pressure loss, a fact that can be justified by the asymmetry of this tape.

Another important analysis is to observe the intensification relation of heat transfer by the associated loss of the optimized configuration. This behavior can be observed by analyzing that the asymmetric configuration of the tape showed an increase in the number of Nusselt, Fig. 7, however, for the optimized configuration the optimization method reduced the total length of the tape and transferred it to an optimal position, so that the pressure loss was reduced. This analysis can also be done through the results shown in Table 7, which represent the longitudinal velocity planes.

Table 7. Velocity field at longitudinal planes.

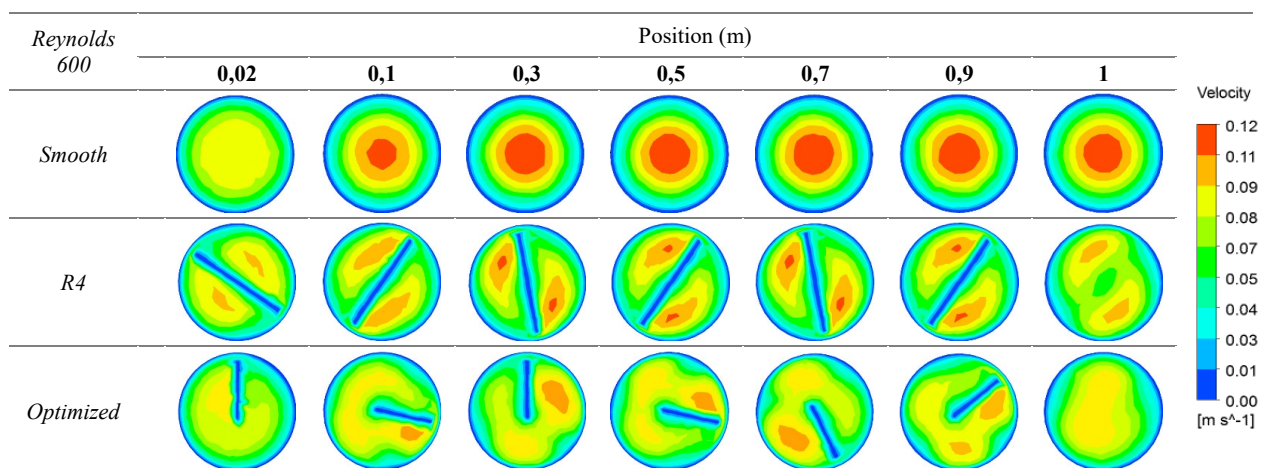


Also in Table 7, it can be seen that while in the Smooth tube and in the twisted tape R4 there is greater uniformity in the flow, the optimized tape has a flow with a higher distortion rate, a characteristic that increases the mixture of the cold and hot streams of the fluid, improving the process of heat transfer in the solar collector, thus, as defined by Vashistha et al.[39], which characterized this phenomenon as the centrifugal forces originated by the movement of distortion of the flow that collide with the heated wall, increasing the transfer of heat by convection.

Another analysis that can be done is related to the low velocity regions for the fluid particles near the wall of the twisted tape. Kumar et al. [40] claim that the presence of the twisted tape blocks the passage of the fluid, which promotes the retardation of the flow.

The thermohydraulic aspects are analyzed from the velocity and temperature fields in transverse planes shown in Tables 8 and 9, where it is possible to analyze the flow in the longitudinal direction.

Table 8. Velocity fields at transverse planes.



The tables shows that for the smooth tube, the behavior of the fluid flow is parabolic, with greater velocity in the center of the cross section, whereas for the tubes with the twisted tape the higher velocity points are located near the torsion zones of the tape where the tangential velocity of the fluid induces axial distortion.

Table 9. Temperature fields at transverse planes.

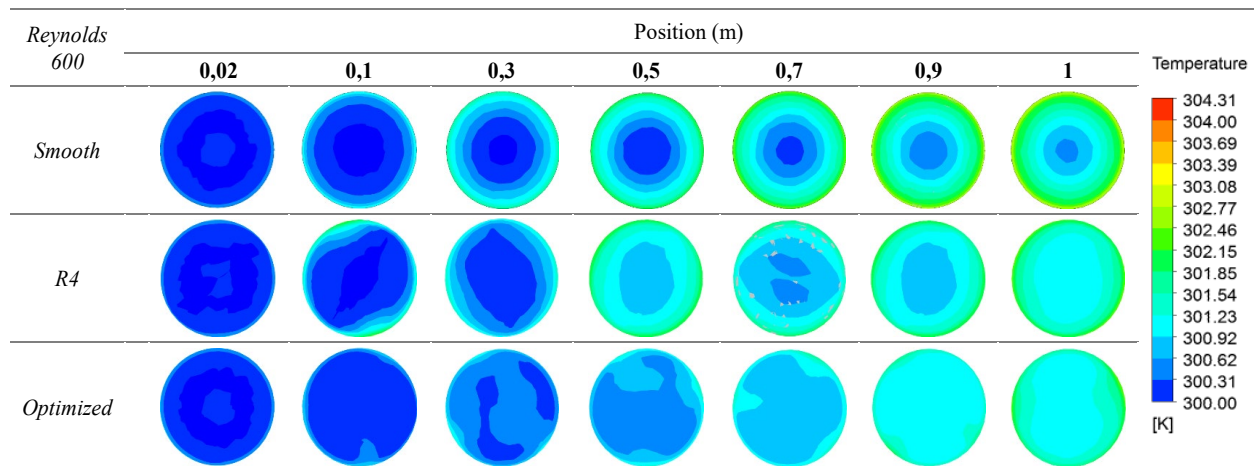
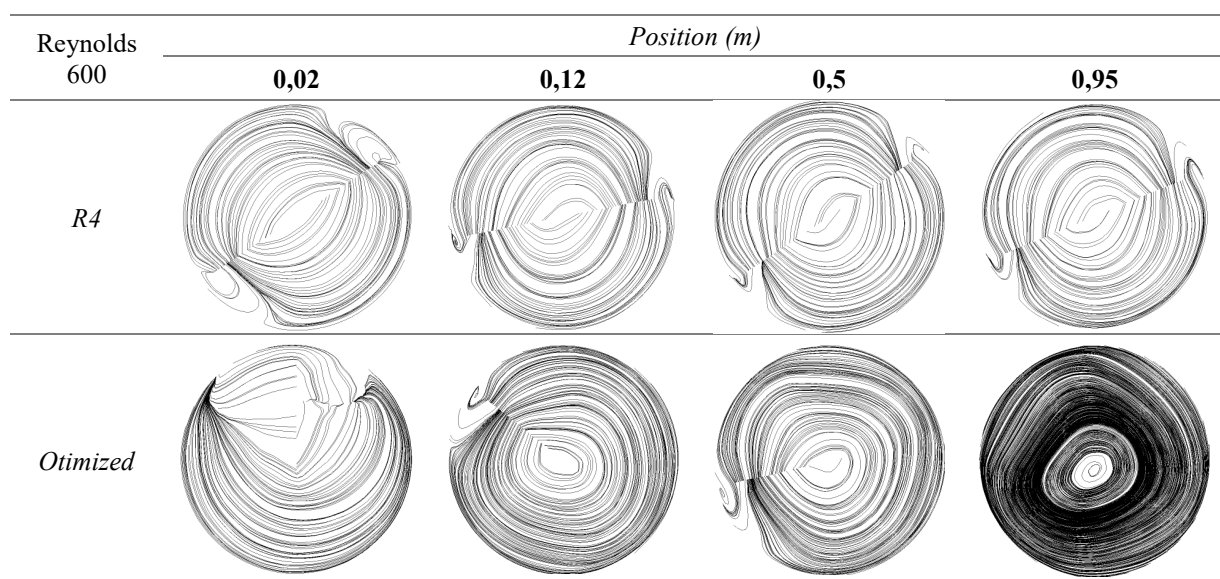


Table 9 show that the optimized twisted tapes produce a significant mixture between the hot and cold fluid streams when compared to the smooth tube temperature fields and the twisted tape R4, promoting a greater intensification of the heat transfer.

Table 10. Stream lines at transverse planes



Twisted tapes create tangential flows that increase hydraulic length and surface contact area [13]. In table 10, can observe the transverse planes of streamlines, where it is possible to identify the axial distortion of the flow and the greater contact between the fluid in the center and the wall of the tube. The distortion promoted by the tapes is responsible for interrupting the development of the thermal boundary layer, which promotes the increase in heat transfer, as well as increase the pressure loss.

4 Conclusions

In this paper an optimization procedure was performed in order to enhance the heat transfer in an active system flat plate solar collector though passive insert known by Twisted Taped. The results developed by the optimization were compared with those of a conventional twisted tape R4, popularly used in the literature to promote increased intensification of heat transfer. The analysis of the

optimization process associated to the heat transfer intensification performance and the associated pressure loss were analyzed numerically by means of the computational modeling and an optimization flowchart carried out in the ANSYS and ESTECO ModeFrontier software, respectively, where it was possible to characterize the dynamics of the flow and the process of intensification of the heat transfer. The geometric parameters associated to the heat transfer intensification and the pressure loss were investigated according to the spatial and geometric characteristics of the twisted tape (Length, Pitch, Radius and Translate) under operating conditions corresponding to the Reynolds number of 600.

The main conclusions found were:

- The results allow concluding that the application of twisted tapes is a very effective technique to enhance the heat transfer in a solar collector operating at low Reynolds number.
- The computational modeling coupling (CFD) to an optimization method (NSGA-II) proved to be an excellent strategy to find optimal solutions in thermal systems. The results for the optimum points generated by the algorithm showed better thermohydraulic performance, as well as characterizing by the asymmetry geometry of the twisted tapes, which demonstrated greater flow distortion, increasing the mixture of the hot and cold streams, maximizing the heat transfer, in addition to decrease the pressure loss compared to a twisted tape R4.
- The optimization process demonstrated excellent results, representing in the Nuf analysis 78 % of the heat transfer enhancement at the increase of the load pressure loss, as twisted tapes with a twist ratio of 4 represent only 41 %. The increase in flow pressure loss was 248 % for the optimized tape while R4 increased by 268 %. Therefore, this data demonstrates that the optimized tape demonstrated better performance compared to the twisted tape R4.

Acknowledgements

The authors acknowledge the grants 2017/17032-3 and 2016/14620-9 of São Paulo Research Foundation (FAPESP) for the scientific initiation and fomentation, respectively.

References

- [1] A. G. Bhave and K. A. Thakare, "Development of a solar thermal storage cum cooking device using salt hydrate," *Sol. Energy*, vol. 171, no. January 2017, pp. 784–789, 2018.
- [2] A. K. Akella, R. P. Saini, and M. P. Sharma, "Social, economical and environmental impacts of renewable energy systems," *Renew. Energy*, vol. 34, no. 2, pp. 390–396, 2009.
- [3] N. L. Panwar, S. C. Kaushik, and S. Kothari, "Role of renewable energy sources in environmental protection: A review," *Renew. Sustain. Energy Rev.*, vol. 15, no. 3, pp. 1513–1524, 2011.
- [4] Ş. Elif, Ş. Can, J. L. Sharp, and A. Anctil, "Factors impacting diverging paths of renewable energy: A review," vol. 81, no. July 2017, pp. 2335–2342, 2018.
- [5] A. H. Mosa, Z. Gha, and L. G. Farshi, "Thermoeconomic assessment of a novel integrated CHP system incorporating solar energy based biogas-steam reformer with methanol and hydrogen production," vol. 178, no. September 2018, pp. 1–16, 2019.
- [6] E. Kabir, P. Kumar, S. Kumar, A. A. Adelodun, and K. Kim, "Solar energy: Potential and future prospects," vol. 82, no. October 2017, pp. 894–900, 2018.
- [7] M. S. Arif, "Residential Solar Panels and Their Impact on the Reduction of Carbon Emissions Mashail S. Arif," pp. 1–18, 2013.
- [8] G. Tsalikis and G. Martinopoulos, "ScienceDirect Solar energy systems potential for nearly net zero energy residential buildings," *Sol. Energy*, vol. 115, no. 2015, pp. 743–756, 2015.
- [9] S. Mekhilef, R. Saidur, and A. Safari, "A review on solar energy use in industries," *Renew. Sustain. Energy Rev.*, vol. 15, no. 4, pp. 1777–1790, 2011.
- [10] K. Hansen and B. V. Mathiesen, "Comprehensive assessment of the role and potential for solar

- thermal in future energy systems,” *Sol. Energy*, vol. 169, no. January, pp. 144–152, 2018.
- [11] M. Mumtaz, A. Khan, N. I. Ibrahim, I. M. Mahbulul, R. Saidur, and F. A. Al-sulaiman, “Evaluation of solar collector designs with integrated latent heat thermal energy storage : A review,” vol. 166, no. February, pp. 334–350, 2018.
- [12] K. Nanan, C. Thianpong, P. Promvongse, and S. Eiamsa-ard, “Investigation of heat transfer enhancement by perforated helical twisted-tapes,” *Int. Commun. Heat Mass Transf.*, vol. 52, pp. 106–112, 2014.
- [13] A. Saravanan, J. S. Senthilkumaar, and S. Jaisankar, “Experimental studies on heat transfer and friction factor characteristics of twist inserted V-trough thermosyphon solar water heating system,” *Energy*, vol. 112, pp. 642–654, 2016.
- [14] S. Sadhishkumar and T. Balusamy, “Performance improvement in solar water heating systems - A review,” *Renew. Sustain. Energy Rev.*, vol. 37, pp. 191–198, 2014.
- [15] P. Samruaisin, W. Changcharoen, C. Thianpong, V. Chuwattanakul, M. Pimsarn, and S. Eiamsa-ard, “Influence of regularly spaced quadruple twisted tape elements on thermal enhancement characteristics,” *Chem. Eng. Process. - Process Intensif.*, vol. 128, no. March, pp. 114–123, 2018.
- [16] S. Eiamsa-ard, K. Yongsiri, K. Nanan, and C. Thianpong, “Heat transfer augmentation by helically twisted tapes as swirl and turbulence promoters,” *Chem. Eng. Process. Process Intensif.*, vol. 60, pp. 42–48, 2012.
- [17] N. Piriyarungrod, M. Kumar, C. Thianpong, M. Pimsarn, V. Chuwattanakul, and S. Eiamsa-ard, “Intensification of thermo-hydraulic performance in heat exchanger tube inserted with multiple twisted-tapes,” *Appl. Therm. Eng.*, vol. 136, no. March, pp. 516–530, 2018.
- [18] C. Zhang *et al.*, “A comparative review of self-rotating and stationary twisted tape inserts in heat exchanger,” *Renew. Sustain. Energy Rev.*, vol. 53, pp. 433–449, 2016.
- [19] S. K. Saha, U. N. Gaitonde, and a. W. Date, “Heat transfer and pressure drop characteristics of turbulent flow in a circular tube fitted with regularly spaced twisted-tape elements,” *Exp. Therm. Fluid Sci.*, vol. 3, no. 6, pp. 632–640, 1990.
- [20] J. Ananth and S. Jaisankar, “Experimental studies on heat transfer and friction factor characteristics of thermosyphon solar water heating system fitted with regularly spaced twisted tape with rod and spacer,” *Energy Convers. Manag.*, vol. 73, pp. 207–213, 2013.
- [21] O. R. Kummitha, V. R. Reddy Bandi, and K. M. Pandey, “3D Numerical Analysis for Thermal-Hydraulic Characteristics of Water Flow Inside a Circular Tube with Twisted Tape with Helical Protrusions,” *Procedia Eng.*, vol. 127, no. December, pp. 1134–1141, 2015.
- [22] Y. Lei, F. Zheng, C. Song, and Y. Lyu, “Improving the thermal hydraulic performance of a circular tube by using punched delta-winglet vortex generators,” *Int. J. Heat Mass Transf.*, vol. 111, pp. 299–311, 2017.
- [23] A. Kumar and B. . Prasad, “Investigation of twisted tape inserted solar water heaters—heat transfer, friction factor and thermal performance results,” *Renew. Energy*, vol. 19, no. 3, pp. 379–398, 2000.
- [24] M. Mirdrikvand, S. Imani Moqadam, B. Roozbehani, and A. Cheshmeh Roshan, *Velocity Boundary Layer Analysis of a Flat Plate Heat Exchanger in Laminar Flow: A Case Study*, vol. 2. 2012.
- [25] B. Van Leer, “Towards the ultimate conservative difference scheme. V. A second-order sequel to Godunov’s method,” *J. Comput. Phys.*, vol. 32, no. 1, pp. 101–136, 1979.
- [26] D. Holmes and S. Connell, “Solution of the 2D Navier-Stokes equations on unstructured adaptive grids,” in *9th Computational Fluid Dynamics Conference*, 1989, p. 1932.
- [27] R. RAUSCH, H. YANG, and J. BATINA, “Spatial adaption procedures on unstructured meshes for accurate unsteady aerodynamic flow computation,” in *32nd Structures, Structural Dynamics, and Materials Conference*, 1991, p. 1106.
- [28] A. Hasanpour, M. Farhadi, and K. Sedighi, “2014 A review study on twisted tape inserts on turbulent flow heat exchangers The overall enhancement ratio criteria.pdf,” vol. 55, pp. 53–62, 2014.
- [29] F. E. Division *et al.*, “Procedure for Estimation and Reporting of Uncertainty Due to Discretization in CFD Applications,” vol. 130, no. July, pp. 128–131, 2008.
- [30] Varun, M. O. Garg, H. Nautiyal, S. Khurana, and M. K. Shukla, “Heat transfer augmentation

- using twisted tape inserts: A review,” *Renew. Sustain. Energy Rev.*, vol. 63, pp. 193–225, 2016.
- [31] L. O. Salviano, D. J. Dezan, and J. I. Yanagihara, “Optimization of winglet-type vortex generator positions and angles in plate-fin compact heat exchanger: Response Surface Methodology and Direct Optimization,” *Int. J. Heat Mass Transf.*, vol. 82, pp. 373–387, 2015.
- [32] H. Holland John, “Adaptation in natural and artificial systems: an introductory analysis with applications to biology, control, and artificial intelligence,” *USA Univ. Michigan*, 1975.
- [33] J. H. Holland, “Genetic algorithms,” *Sci. Am.*, vol. 267, no. 1, pp. 66–73, 1992.
- [34] D. E. Goldberg, “Genetic algorithms in search, optimization, and machine learning, addison-wesley, reading, ma, 1989,” *Google Sch.*, 2014.
- [35] C. Z. Janikow and Z. Michalewicz, “An experimental comparison of binary and floating point representations in genetic algorithms,” in *ICGA*, 1991, pp. 31–36.
- [36] P. J. Fleming and R. C. Purshouse, “Evolutionary algorithms in control systems engineering: a survey,” *Control Eng. Pract.*, vol. 10, no. 11, pp. 1223–1241, 2002.
- [37] K. Deb, A. Pratap, S. Agarwal, and T. Meyarivan, “A fast and elitist multiobjective genetic algorithm: NSGA-II,” *IEEE Trans. Evol. Comput.*, vol. 6, no. 2, pp. 182–197, 2002.
- [38] A. Lemouedda, M. Breuer, E. Franz, T. Botsch, and A. Delgado, “Optimization of the angle of attack of delta-winglet vortex generators in a plate-fin-and-tube heat exchanger,” *Int. J. Heat Mass Transf.*, vol. 53, no. 23–24, pp. 5386–5399, 2010.
- [39] C. Vashistha, A. K. Patil, and M. Kumar, “Experimental investigation of heat transfer and pressure drop in a circular tube with multiple inserts,” *Appl. Therm. Eng.*, vol. 96, pp. 117–129, 2016.
- [40] B. Kumar, G. P. Srivastava, M. Kumar, and A. K. Patil, “A review of heat transfer and fluid flow mechanism in heat exchanger tube with inserts,” *Chem. Eng. Process. Process Intensif.*, vol. 123, no. November 2017, pp. 126–137, 2018.